Applied Catalysis B: Environmental 130–131 (2013) 25–35

Contents lists available at SciVerse ScienceDirect

Applied Catalysis B: Environmental

journal homepage: www.elsevier.com/locate/apcatb

NH_3 decomposition and oxidation over noble metal-based FCC CO combustion promoters

Behnam Bahrami[a], Vasileios G. Komvokis[a], Michael S. Ziebarth[b], Oleg S. Alexeev[a,**], Michael D. Amiridis[a,*]

[a] Department of Chemical Engineering, University of South Carolina, Columbia, SC 29208, United States
[b] Grace Davison Refining Technologies, Columbia, MD 21044, United States

ARTICLE INFO

Article history:
Received 12 August 2012
Received in revised form
27 September 2012
Accepted 28 September 2012
Available online 11 October 2012

Keywords:
NO_x reduction
NH_3 oxidation
FCC additives
Palladium
Platinum
Rhodium
Nitrates
Nitrites

ABSTRACT

The surface chemistry of NH_3 decomposition and oxidation was examined over $M^{n+}/Ce^{n+}/Na^+/\gamma\text{-}Al_2O_3$ commercial catalysts incorporating Pt, Pd, and Rh in order to clarify the role of these materials in converting NH_3 into N_2 and NO_x within the dense phase of FCC regenerators. All catalysts were active in promoting the decomposition of NH_3 into N_2 in the 500–700 °C temperature range, with the Rh containing catalyst being the most active at 700 °C. Oxygen species activated on the surfaces of these materials significantly enhanced the selective conversion of NH_3 into N_2. When O_2 was present in the feed, complete conversion of NH_3 – with approximately 80% selectivity to N_2 – was observed over the reduced Pt-, Pd-, and Rh-containing materials at temperatures as low as 200, 300, and 350 °C, respectively. At temperatures below 350 °C, the NH_3 oxidation reaction follows an iSCR-type pathway, in which a fraction of NH_3 is converted into NO_x and subsequently into surface nitrite/nitrate species capable of reacting with the remaining portion of NH_3 to form N_2. Although the oxidation of NH_3 to NO_x prevails at 700 °C under excess O_2 conditions, optimal O_2 concentrations can be found under which both complete NH_3 conversion and high N_2 selectivity are achieved. Under these conditions, the noble metal component of the $M^{n+}/Ce^{n+}/Na^+/\gamma\text{-}Al_2O_3$ materials promotes the reaction of NH_3 with the NO_x formed, yielding N_2. Excess O_2 effectively hinders this reaction pathway at high temperatures. Overall, the results presented herein indicate that the significant increase in NO_x emissions, typically observed over conventional Pt-based FCC CO combustion promoters, could be directly attributed to the oxidation of NH_3 formed in the reducing zone of the FCC regenerators.

1. Introduction

Fluid catalytic cracking (FCC) technology is currently used in petroleum refineries to convert heavy oil feedstocks into lighter products, such as diesel, gasoline, and light olefins [1]. Since strict regulations are currently in place to control emissions from refineries [2], this otherwise mature technology is facing new challenges associated with the reduction of CO, SO_x, and NO_x emissions. FCC units are responsible for approximately 50% of NO_x emissions from refineries [3,4]. The presence of nitrogen-containing compounds in the crude oil explains the appearance of NO_x emissions during the FCC catalyst regeneration process since a significant fraction (approximately 5%) of the nitrogen from the crude oil ends up in the coke accumulated on the catalyst during the cracking process in the riser [2–4]. The concentration of NO_x released from FCC regenerators depends primarily on the regenerator design and the operating conditions used [4]. In addition to NO_x, the FCC regenerator exhaust may also contain HCN and NH_3 if the regenerator is operated at partial burn [4,5]. In this case, HCN and NH_3 are further converted into NO_x in the CO boiler located downstream from the regenerator [4,5]. Typically, ammonia is observed in larger amounts than HCN since the latter can be easily converted to NH_3 by hydrolysis in the presence of H_2O [5]. This reaction has been examined extensively over various oxides and it has been shown that even unpromoted oxides such as CaO, Al_2O_3, TiO_2, and ZrO_2 are capable of catalyzing it to different degrees in the 250–500 °C temperature range with a maximum activity observed at approximately 500 °C [6–9]. In fact, it has been suggested that the hydrolysis of HCN may be taking place over the oxide phases present in the matrix (clays, mixed aluminum oxides, etc.) of the FCC catalyst [7]. Catalysts incorporating Pd or Pt exhibit substantially higher activities for the hydrolysis of HCN [8]. No HCN or NH_3 emissions are observed when the regenerator is

* Corresponding author. Tel.: +1 803 7772808; fax: +1 803 7779502.
** Corresponding author. Tel.: +1 803 7779914; fax: +1 803 7778265.
E-mail addresses: alexeev@cec.sc.edu (O.S. Alexeev), amiridis@mailbox.sc.edu (M.D. Amiridis).

0926-3373/$ – see front matter © 2012 Elsevier B.V. All rights reserved.
http://dx.doi.org/10.1016/j.apcatb.2012.09.057

operated under full burn conditions (i.e., when greater than stoichiometric amounts of air are used to burn off the coke) because these species are converted to NO_x and N_2 [4,5].

Noble metal-based catalytic additives are currently used in most refineries to reduce the CO emissions from FCC regenerators in situ [10]. However, these additives significantly increase NO_x emissions as well [1,2,11]. Developing new formulations of FCC additives capable of providing simultaneous reduction of CO and NO_x emissions has been a research focus for FCC catalyst manufacturers. Catalytic formulations incorporating Pd and CeO_2 have been used as an alternative to Pt, and such formulations were found to be effective for the reduction of NO_x under FCC regenerator conditions [12–15]. However, the reasons as to why more NO_x is generated over Pt than Pd in FCC regenerators remain largely unknown.

The answer to this question is hidden in the complex nitrogen chemistry taking place under FCC regenerator conditions. This chemistry is not fully understood and the relative contributions of various nitrogen-containing intermediates to the overall network of chemical reactions, leading to the formation and reduction of NO_x, remain mostly unknown. However, several reports can be found in the literature indicating the importance of such intermediate species. For example, it has been suggested that the coke-bound nitrogen is initially converted into HCN and NH_3 which are further converted into NO_x and N_2 via a sequence of gas phase reactions [16]. In addition, it has been suggested that when Pt is present in the catalyst formulation, it plays a significant role in the oxidation of HCN and NH_3 to NO_x [1,7,16]. More recent information available in several patents suggests that NH_3 is an important intermediate in the NO_x formation and reduction chemistry under FCC regenerator conditions [17,18]. Along these lines, it is easy to envision how NH_3 can undergo partial or full oxidation or participate in reactions with NO_x and CO under the variety of FCC regenerator conditions applied in the field. However, to the best of our knowledge, the question as to how different FCC additives affect these chemical transformations of NH_3 remains largely unexplored.

In our previous reports [19–21] we have examined the structure of $Pd^{n+}/Ce^{n+}/Na^{+}/\gamma\text{-}Al_2O_3$-type materials under oxidizing and reducing conditions; we have determined how each component of these materials interacts with NO_x, CO, and NH_3 at elevated temperatures; and we have examined the $CO + NO_x$, $NO_x + O_2$, $NH_3 + O_2$, and $NH_3 + CO$ reactions taking place on the surfaces of these materials under conditions approaching those existing in FCC regenerators.

In this work, we focus on the chemistry of NH_3 oxidation taking place on surfaces of noble metal-based CO combustion promoters with a $M^{n+}/Ce^{n+}/Na^{+}/\gamma\text{-}Al_2O_3$ (M = Pd, Pt, Rh) general composition. By combining previous in situ FTIR results with current steady state kinetic measurements, we address (1) the nature of surface intermediates formed, as well as their reactivity and thermal stability, (2) the contribution of different reactions to the overall NH_3 oxidation reaction network, and (3) the relative effect of the different noble metals on the surface reactions occurring under FCC regenerator conditions.

2. Experimental

2.1. Reagents and materials

Aluminum oxide with a BET surface area of 200 m^2/g was prepared by calcination of an acid peptizable boehmite aluminum oxide hydroxide material (Capital B, SASOL) at 600 °C and was used as the catalyst support. Palladium, rhodium, and tetraaminoplatinum nitrate solutions (all Alfa Aesar) were used as received for the preparation of catalysts. He and NO/He, NH_3/He, and O_2/He mixtures (all UHP grade; Airgas) were used as supplied.

2.2. Sample preparation

The $Ce^{n+}/Na^{+}/Al_2O_3$ material, with a BET surface area of 110 m^2/g and nominal Na_2O and CeO_2 loadings of 7 and 20 wt.%, respectively, was prepared as described elsewhere [20]. Samples incorporating Pd, Pt, or Rh were prepared by incipient wetness impregnation of the $Ce^{n+}/Na^{+}/Al_2O_3$ material with an aqueous solution of the corresponding metal precursor. The amount of each precursor was chosen to yield samples containing 0.1 wt.% Pd, 0.05 wt.% Rh, or 0.025 wt.% Pt. These metal loadings were chosen based on the market value of each metal (at the time when this work was initiated) with the goal of keeping the total cost of catalytic materials approximately the same. After the impregnation step was completed, all samples were dried in air at 200 °C for 24 h and then calcined at 650 °C for 2 h.

2.3. Kinetic measurements

All kinetic measurements were performed in a quartz single-pass fixed-bed reactor at atmospheric pressure and temperatures in the 100–700 °C range. The temperature inside the reactor was monitored by a thermocouple extended into the catalyst bed. Samples in powder form (0.2 g) were diluted 15 times by weight with quartz particles (60–80 mesh) to keep the catalyst bed isothermal. The total volumetric flow rate of the reactant mixture (i.e., 500 ppm NH_3/He for ammonia decomposition experiments or 500 ppm NH_3/200–2500 ppm O_2/He for ammonia oxidation experiments) was chosen in each case to yield a corresponding Gas Hourly Space Velocity (GHSV) of 29×10^6 ml/mol of metal h. The feed and the reaction products were analyzed with an on-line single beam NDIR NO_x analyzer (ZRF, California Analytic Instruments) capable of detecting NO_x in the 0–1800 ppm range and with an online HP 5890 gas chromatograph (Hewlett Packard) equipped with a thermal conductivity detector (TCD) and two columns (i.e., Porapak Q and molecular sieves).

Prior to catalytic measurements, all samples were treated with either 1% O_2/He or 10% H_2/He while the temperature was ramped at 5 °C/min from 25 to 550 °C and held at the final temperature for 3 h. After this treatment was completed, the reactor was purged at the final temperature with He for 1 h and cooled to 100 °C under He flow. The reaction mixture was introduced at that point and data were collected as a function of time, while the reaction temperature was increased every 2 h in 50 °C increments. In the absence of a catalyst, there was no measurable conversion of NH_3.

The NH_3 conversion (X) was calculated based on the formation of nitrogen-containing products as: $X = \left(\sum n_i p_i / [NH_3]_0\right) \times 100\%$, where p_i is the molar concentration for the specific product (i), n_i is the number of N atoms in each product, and $[NH_3]_0$ is the initial concentration of NH_3 in the feed. The selectivity was defined as the percentage of NH_3 converted to the specific product (i) over the total NH_3 consumed.

3. Results and discussion

When NH_3 is formed in FCC regenerators operating under different combustion modes, it can undergo further transformations over the surfaces of the $M^{n+}/Ce^{n+}/Na^{+}/\gamma\text{-}Al_2O_3$ (where M = Pd, Pt, and Rh) additives. Moreover, both oxidized and reduced forms of these materials are expected to be present within the dense phase of the regenerator under partial burn conditions. Therefore, we first examined the reactivity of NH_3 in the 400–700 °C range over these materials in the absence of any other reactant in the feed.

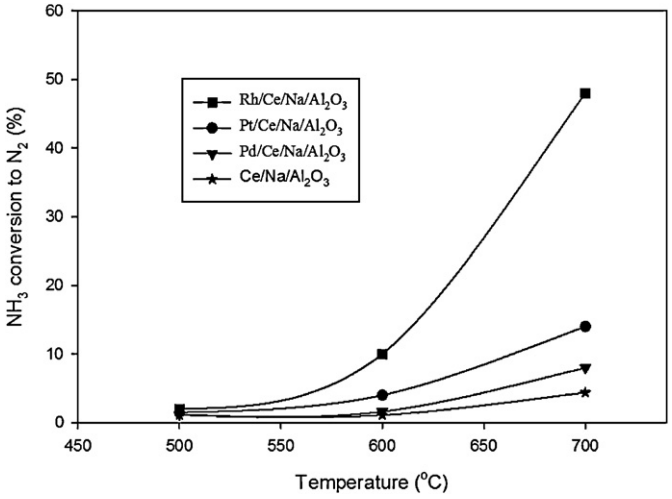

Fig. 1. Conversion of NH_3 to N_2 as a function of temperature over different $M/Ce^{n+}/Na^+/\gamma\text{-}Al_2O_3$ materials treated in H_2 at 550 °C (feed composition: 500 ppm NH_3/He).

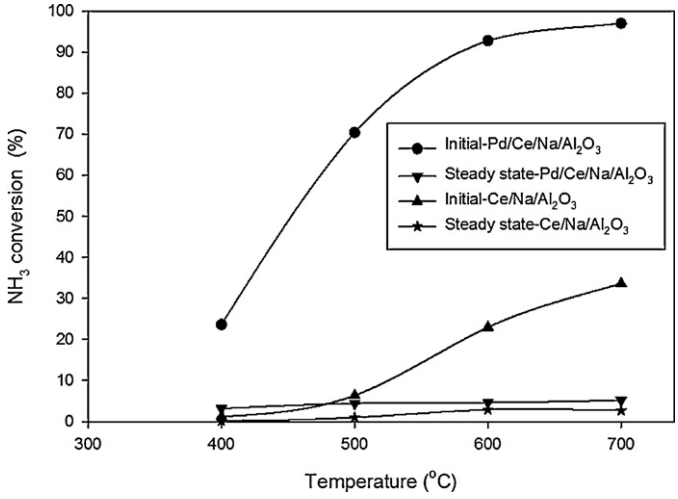

Fig. 2. Initial and steady state conversions of NH_3 to N_2 as a function of temperature over $Pd^{n+}/Ce^{n+}/Na^+/\gamma\text{-}Al_2O_3$ and $Ce^{n+}/Na^+/\gamma\text{-}Al_2O_3$ materials treated in O_2 at 550 °C (feed composition: 500 ppm NH_3/He).

3.1. NH_3 reactivity over reduced $M/Ce^{n+}/Na^+/\gamma\text{-}Al_2O_3$

When reduced $M/Ce^{n+}/Na^+/\gamma\text{-}Al_2O_3$ materials were exposed to a 500 ppm NH_3/He mixture at different temperatures, a measurable conversion of ammonia to nitrogen was observed at temperatures above 500 °C for all samples examined (Fig. 1). In all cases, a steady state behavior is reached after a few minutes of exposure and no signs of deactivation were detected during the first 120 min on stream. No other nitrogen-containing products were detected in the effluent, indicating that ammonia is converted exclusively to N_2 under these conditions. Regardless of the type of noble metal used in the formulation, all reduced samples exhibit approximately the same low activity for the conversion of NH_3 at temperatures below 600 °C and show no substantial difference in performance when compared with the $Ce^{n+}/Na^+/\gamma\text{-}Al_2O_3$ support, suggesting that the support itself is the main contributor to the reaction.

FTIR results reported previously indicate that ammonia readily adsorbs on the $Ce^{n+}/Na^+/\gamma\text{-}Al_2O_3$ surface at low temperatures and undergoes decomposition even at 100 °C, yielding NH_x intermediates [21]. Furthermore, the appearance of NO_2^- species in traceable amounts on the same material takes place in the 400–600 °C temperature range when the NH_x species are further oxidized by oxygen from the support to yield nitrites. The role of the lattice oxygen atoms in the conversion of NH_3 over surfaces of various metal oxides has been emphasized in several publications. For example, it has been reported that Cr_2O_3 lattice oxygen is capable of participating in the sequential abstraction of hydrogen from ammonia to form NH_x intermediates and eventually nitrogen atoms [22]. At temperatures above 550 °C, the latter not only recombine to form N_2, but can also replace oxygen atoms in the Cr_2O_3 lattice to form CrN_xO_y defects, which are believed to be the active sites for further ammonia decomposition. Similar to the role of lattice oxygen in the selective oxidation of hydrocarbons [23,24], some other reports suggest that NH_3 can be oxidized to NO_x by lattice oxygen with the latter then reacting with ammonia to form N_2 [25,26].

The catalytic performance of the Pt- and Pd-containing formulations was found to be similar in the 600–700 °C temperature range, while the difference with the performance of the $Ce^{n+}/Na^+/\gamma\text{-}Al_2O_3$ support was relatively small (Fig. 1). This result suggests that at the low metal loadings used, both these metals do not contribute substantially to the NH_3 decomposition process in the reduced form. In contrast, the conversion of NH_3 to N_2 was found to be as high as 10% at 600 °C and 48% at 700 °C over the Rh-based formulation, consistent with other literature reports indicating that Rh is more active than Pt and Pd for NH_3 decomposition at temperatures up to 750 °C [27,28]. Previous DFT calculations suggest that the higher activity of Rh over Pt and Pd in ammonia decomposition is associated primarily with the lower activation barrier for the first proton abstraction step and with the enhanced stabilization of the various NH_x intermediates involved [29]. Once the NH_3 dissociation process is completed, the recombination of N and H atoms to N_2 and H_2 is energetically favored on metal surfaces [28]. Consistent with these literature examples, our activity data clearly show that even at the very low Rh loading levels used (i.e., 0.05 wt.%), the presence of reduced Rh species in the $Rh/Ce^{n+}/Na^+/\gamma\text{-}Al_2O_3$ material favors the NH_3 decomposition process in the 600–700 °C temperature range and significantly promotes the baseline activity of the $Ce^{n+}/Na^+/\gamma\text{-}Al_2O_3$ support.

3.2. NH_3 reactivity over oxidized $M^{n+}/Ce^{n+}/Na^+/\gamma\text{-}Al_2O_3$

As we reported previously, treatment of the $M/Ce^{n+}/Na^+/\gamma\text{-}Al_2O_3$ materials with 1% O_2/He at 550 °C results in complete oxidation of the metal component [19]. Furthermore, the catalytic behavior of all oxidized $M^{n+}/Ce^{n+}/Na^+/\gamma\text{-}Al_2O_3$ samples was found to be similar. Therefore, the catalytic activity data shown in Fig. 2 and Table 1 are limited to $Pd^{n+}/Ce^{n+}/Na^+/\gamma\text{-}Al_2O_3$ and $Ce^{n+}/Na^+/\gamma\text{-}Al_2O_3$ for brevity.

When the $Ce^{n+}/Na^+/\gamma\text{-}Al_2O_3$ support was pretreated in a 1% O_2/He mixture at 550 °C and then exposed to the 500 ppm NH_3/He flow at different temperatures, a measurable conversion of ammonia was first observed at approximately 400 °C (Fig. 2). Since this temperature is approximately 100 °C lower than that in the case of the same sample pretreated in H_2, it is apparent that the pretreatment with O_2 promotes the conversion of NH_3. The total initial conversion of NH_3 over this material was found to be as high as 34% at 700 °C. In this case, however, the conversion of NH_3 declines significantly with time on stream at all temperatures examined, coming to a steady state after approximately 30 min of exposure and showing no further deactivation signs thereafter. The steady state conversion is approximately equal to what was observed for the reduced sample. Both N_2 and NO_x species were detected in the effluent during the initial period of time, but only N_2 was formed after steady state was reached (Table 1).

It has been reported previously that oxides of different metals, including alumina, are capable of activating oxygen species in

Table 1
Ammonia conversion at 700 °C over reduced and oxidized samples (feed composition: 500 ppm NH_3/He).

Sample	Treatment	Initial NH_3 conversion (%)			Steady state NH_3 conversion (%)		
		Total	to N_2	to NO	Total	to N_2	to NO
$Ce^{n+}/Na^+/\gamma\text{-}Al_2O_3$	O_2/He 550 °C	34	27	7	3	3	–
	H_2/He 550 °C	4	4	–	4	4	–
$Pd^{n+}/Ce^{n+}/Na^+/\gamma\text{-}Al_2O_3$	O_2/He 550 °C	97	90	7	6	6	–
	H_2/He 550 °C	8	8	-	8	8	–

various forms on their surfaces [30]. Furthermore, while CeO_2 is known to exhibit high oxygen storage and release capacities [31], the presence of Na_2O has also been found to increase the rate of oxygen dissociation [32,33]. Since the $Ce^{n+}/Na^+/\gamma\text{-}Al_2O_3$ support incorporates both of these components in substantial concentrations, the oxygen species activated by them during the high temperature treatment in the O_2/He mixture are most likely responsible for the high initial conversion of NH_3. Since both N_2 and NO species were detected in the effluent, it is evident that the NH_3 oxidation process includes the following general reactions in which O_s represents oxygen species activated by the support:

$$2NH_3 + 3O_s = N_2 + 3H_2O \quad (1)$$

$$2NH_3 + 5O_s = 2NO + 3H_2O \quad (2)$$

The initial NH_3 conversions values shown in Table 1 further suggest that at 700 °C the majority of NH_3 is converted via reaction (1), while the contribution of reaction (2) is relatively low. Furthermore, the results of Fig. 2 and Table 1 indicate that when all activated oxygen species are consumed and steady state is reached, the thermal decomposition of ammonia is the primary pathway for the formation of N_2 and no substantial differences are observed at this point between the catalytic properties of the oxidized and reduced $Ce^{n+}/Na^+/\gamma\text{-}Al_2O_3$ samples.

The activity data obtained for the $Pd^{n+}/Ce^{n+}/Na^+/\gamma\text{-}Al_2O_3$ sample pretreated in 1% O_2/He at 550 °C (Fig. 2) further demonstrate that the initial NH_3 conversions over this material are substantially higher than those observed over the $Ce^{n+}/Na^+/\gamma\text{-}Al_2O_3$ support in the whole range of temperatures examined. It is further evident that substantially more N_2 was formed over $Pd^{n+}/Ce^{n+}/Na^+/\gamma\text{-}Al_2O_3$, as the initial conversion of NH_3 to N_2 was found to be approximately 90% at 700 °C (Table 1). At the same time, the initial formation of NO_x remains approximately the same as in the case of the $Ce^{n+}/Na^+/\gamma\text{-}Al_2O_3$ support (Table 1), indicating that the support is the main contributor to the formation of NO_x, while the palladium oxide component promotes substantially the conversion of NH_3 to N_2.

It has been reported previously that the presence of NiO on the Ni (1 1 1) surface does not affect the reactivity of NH_3 but oxygen species preadsorbed on the Ni (1 1 1) surface have a very strong effect [34]. However, it is very unlikely that the PdO component substantially promotes the activation of oxygen species on the $Ce^{n+}/Na^+/\gamma\text{-}Al_2O_3$ surface, because DFT calculations predict that PdO is not capable of dissociating molecular oxygen [35]. It has also been reported that lattice oxygen of $\gamma\text{-}Al_2O_3$-supported CuO species is capable of reacting with NH_3 to produce N_2, with the $[Cu{-}O{-}Cu]^{2+}$ fragments in the CuO structure representing the active sites [36]. If one assumes that the PdO component incorporates somewhat similar sites that promote the conversion of NH_3 to N_2, it becomes unclear as to why the activity of the $Pd^{n+}/Ce^{n+}/Na^+/\gamma\text{-}Al_2O_3$ material sharply drops with time on stream at all examined temperatures. It is more likely that the transient catalytic behavior exhibited by the $Pd^{n+}/Ce^{n+}/Na^+/\gamma\text{-}Al_2O_3$ sample pretreated in O_2 is related to the redox properties of the PdO component. TPR data available in the literature [37–39] show that PdO species supported on various metal oxide supports can be completely reduced to metallic Pd by H_2 in the 25–150 °C temperature range, depending on their dispersion. Since the $Pd^{n+}/Ce^{n+}/Na^+/\gamma\text{-}Al_2O_3$ material incorporates the PdO component in a highly dispersed state, it is likely that the hydrogen species generated on the surface of this material during the decomposition of NH_3 are readily reducing the entire amount of PdO according to the following stoichiometry:

$$2NH_3 + 3PdO = 3Pd + N_2 + 3H_2O \quad (3)$$

Based on this stoichiometry and the amount of PdO present in the $Pd^{n+}/Ce^{n+}/Na^+/\gamma\text{-}Al_2O_3$ sample, one can calculate that approximately 309 ppm of NH_3 will suffice for this reaction, yielding 155 ppm of N_2. Given that the initial conversion of NH_3 to N_2 over the $Ce^{n+}/Na^+/\gamma\text{-}Al_2O_3$ support is approximately 27%, this additional generation of N_2 is expected to elevate the total NH_3 conversion to approximately 90%, which is consistent with the experimentally determined value reported in Table 1 for the Pd-based formulation. In the absence of any additional sources of O_2, the reduction of PdO species by NH_3 is evidently a stoichiometric process. Furthermore, the results shown in the previous section (Section 3.1) clearly demonstrate that the Pd component in the reduced form does not substantially contribute to the NH_3 decomposition process. This explains why after the reduction of the PdO species is completed and steady state is reached, the catalytic performance of the oxidized $Pd^{n+}/Ce^{n+}/Na^+/\gamma\text{-}Al_2O_3$ material becomes indistinguishable from that of the reduced sample and the $Ce^{n+}/Na^+/\gamma\text{-}Al_2O_3$ support (Table 1).

In summary, experiments with reduced and oxidized $M^{n+}/Ce^{n+}/Na^+/\gamma\text{-}Al_2O_3$ materials clearly show that NH_3 can undergo decomposition/oxidation on their surfaces to form N_2. Under reducing conditions and temperatures approaching those existing in FCC regenerators, the contribution of this reaction is low in the case of the Pd- and Pt-containing samples. In contrast, the Rh-containing sample was found to be more active for the NH_3 decomposition/oxidation reaction with the conversion of NH_3 to N_2 being as high as 48% at 700 °C. The pretreatment of $M/Ce^{n+}/Na^+/\gamma\text{-}Al_2O_3$ materials in oxygen substantially promotes the initial conversion of NH_3 to N_2. However, when steady state is reached after a few minutes of NH_3 exposure, the catalytic properties of the prereduced and preoxidized samples become identical, indicating that oxygen species activated and/or stored on the surface of these materials during the pretreatment are responsible for the promotional effect. It is further evident that this surface oxygen-assisted decomposition of NH_3 proceeds at a higher rate when oxides of noble metals are present on the surface. The role of the noble metal oxide component is to scavenge the hydrogen atoms formed during the NH_3 decomposition process (reaction (3)). In the absence of any additional oxygen sources, this reaction is very selective to N_2 and does not generate NO_x species even at temperatures as high as 700 °C.

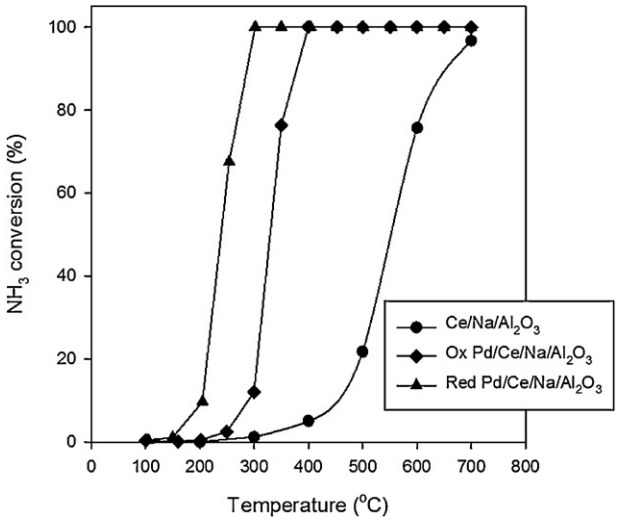

Fig. 3. Conversion of NH_3 as a function of temperature over $Ce^{n+}/Na^+/\gamma\text{-}Al_2O_3$ and $Pd^{n+}/Ce^{n+}/Na^+/\gamma\text{-}Al_2O_3$ materials exposed to a 2500 ppm O_2/500 ppm NH_3/He mixture.

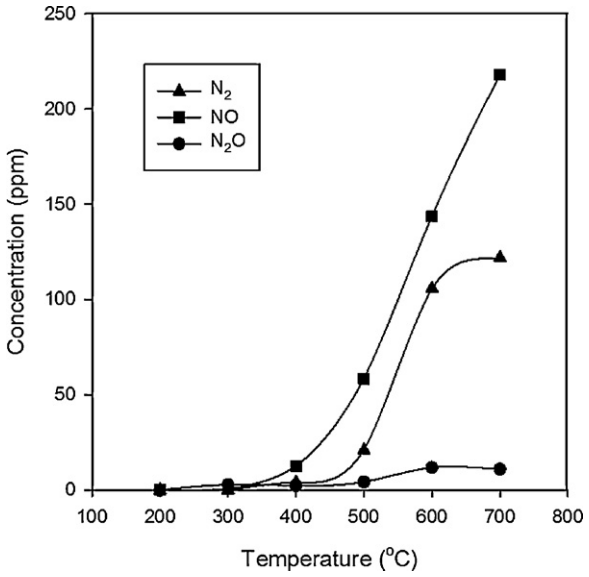

Fig. 4. Product distribution of NH_3 oxidation as a function of temperature over the $Ce^{n+}/Na^+/\gamma\text{-}Al_2O_3$ material (feed composition: 2500 ppm O_2/500 ppm NH_3/He).

3.3. Reaction of NH_3 with O_2 over $M^{n+}/Ce^{n+}/Na^+/\gamma\text{-}Al_2O_3$ materials

When FCC regenerators operate under partial or full burn conditions, the distribution of O_2 through the dense phase of the regenerator is not uniform [3,4]. Therefore, different zones ranging from a reducing environment and a complete lack of O_2 to a fully oxidizing environment are present in the unit. Since the concentration of O_2 varies significantly in such zones, it is desirable to understand how both the conversion of NH_3 and the product distribution vary with the O_2 concentration. To further investigate these issues, the activity measurements described in the previous sections were repeated using O_2/500 ppm NH_3/He mixtures with variable concentrations of oxygen.

3.3.1. Oxidation of NH_3 under excess O_2 conditions

Fig. 3 shows the conversion of NH_3 as a function of temperature over $Ce^{n+}/Na^+/\gamma\text{-}Al_2O_3$ and $Pd^{n+}/Ce^{n+}/Na^+/\gamma\text{-}Al_2O_3$ materials exposed to a 2500 ppm O_2/500 ppm NH_3/He mixture. Prior to these experiments, the $Pd^{n+}/Ce^{n+}/Na^+/\gamma\text{-}Al_2O_3$ material was pretreated either in a 10% H_2/He or a 1% O_2/He mixture at 550 °C for 3 h and then purged with He at the same temperature in order to investigate any differences in the catalytic performance related to the initial state of Pd. In the case of the prereduced sample, the first measurable conversion of NH_3 was observed at 150 °C with complete conversion observed at approximately 300 °C. The conversion curve characterizing the same sample pretreated in a 1% O_2/He mixture is shifted to higher temperatures by approximately 100 °C, indicating that the oxidized sample is significantly less active in this reaction than the reduced one. The $Ce^{n+}/Na^+/\gamma\text{-}Al_2O_3$ support is also capable of converting NH_3 under these conditions at temperatures above 350 °C with 97% NH_3 conversion reached at 700 °C, a temperature at which most FCC regenerators operate. Evidently, the overall activity of the $Ce^{n+}/Na^+/\gamma\text{-}Al_2O_3$ support for NH_3 oxidation is significantly lower in the absence of Pd since the conversion curve for this sample is further shifted to higher temperatures by approximately 230 °C. The significant differences in the NH_3 oxidation activity observed between the $Ce^{n+}/Na^+/\gamma\text{-}Al_2O_3$ and Pd-containing samples, as well as the differences observed between preoxidized and prereduced Pd-containing materials demonstrate that both the presence of the noble metal component and its oxidation state play a crucial role in this reaction.

Since the activity measurements show that the rate of NH_3 oxidation is significantly enhanced at low temperatures over the reduced $Pd/Ce^{n+}/Na^+/\gamma\text{-}Al_2O_3$ material (Fig. 3), we can conclude that reduced Pd particles are more active in this reaction than PdO species. This conclusion is consistent with other literature reports demonstrating a similar trend. For example, it has been reported that the H_2 treatment of a $PdO/\gamma\text{-}Al_2O_3$ sample significantly increases the low temperature NH_3 oxidation activity of this catalyst [40]. Similarly, during the NH_3-SCR reaction, an oxidized AgO_x/Al_2O_3 sample was found to be less active than the corresponding reduced one [41,42]. The same pattern was also observed for the CH_4 oxidation reaction over $PdO/\gamma\text{-}Al_2O_3$ and PdO/ZrO_2 catalysts [43–46]. While strong metal oxide–support interactions were suggested to be responsible for the relatively low activity of the oxidized samples in some of these reports [46], other literature data suggest that oxygen species activated by the reduced metal surfaces are much more reactive than those incorporated into metal oxide structures [41,42]. Even though the feed composition used in our experiments (i.e., 2500 ppm O_2/500 ppm NH_3/He) is net oxidizing, it is expected that at least some fraction of Pd will remain in the reduced state under reaction conditions at relatively low temperatures and low NH_3 conversions. Since reduced Pd surfaces are capable of dissociating O_2 species [47–50], this could reasonably explain the superior activity of the reduced $Pd^{n+}/Ce^{n+}/Na^+/\gamma\text{-}Al_2O_3$ sample for NH_3 oxidation. It should be further mentioned that Pt- and Rh-containing formulations pre-treated in oxygen or hydrogen show the same type of the catalytic behavior as Pd for NH_3 oxidation. Activity measurements characterizing these materials are shown in Figs. 1S and 3S of the supporting information.

Fig. 4 shows the product distribution of NH_3 oxidation as a function of temperature over the $Ce^{n+}/Na^+/\gamma\text{-}Al_2O_3$ support. In this case, the reaction products appear only at temperatures above 300 °C and their concentration in the effluent increases progressively with temperature until the conversion of NH_3 reaches its maximum at 700 °C. NO_x appears in the effluent in larger concentrations than N_2 in the whole range of examined temperatures and the selectivities of these products at 700 °C were found to be 47 and 53%, respectively. The formation of NO_x and N_2 from NH_3 dominate the surface chemistry over the $Ce^{n+}/Na^+/\gamma\text{-}Al_2O_3$ support and can in general be described as follows:

$$4NH_3 + 5O_2 = 4NO + 6H_2O \quad (4)$$

$$4NH_3 + 3O_2 = 2N_2 + 6H_2O \quad (5)$$

At the high temperatures typically present in FCC regenerators, NO_x species formed in reaction (4) could further decompose to produce N_2. However, the contribution of this process to the overall N_2 selectivity is evidently low because separate experiments performed with the $Ce^{n+}/Na^+/\gamma\text{-}Al_2O_3$ material and a 750 ppm NO/He feed revealed that the conversion of NO_x to N_2 does not exceed 2% at 700 °C. Therefore, this material is not capable of catalyzing the decomposition of nitric oxide even in the absence of O_2. However, it is also possible that the reaction of NH_3 with NO_x formed in reaction (4) can be responsible for the formation of N_2:

$$4NH_3 + 6NO = 5N_2 + 6H_2O \quad (6)$$

A different depiction of the same reaction also combines reactions (4) and (6) as follows:

$$4NH_3 + 4NO + O_2 = 4N_2 + 6H_2O \quad (7)$$

Experiments performed with a 500 ppm NH_3/750 ppm NO/He mixture indeed show that reaction (6) takes place without any deactivation over the $Ce^{n+}/Na^+/\gamma\text{-}Al_2O_3$ material at 700 °C with approximately 40% of NO_x converted to N_2 (Fig. 5). However, when 2500 ppm of O_2 was added to the NH_3/NO_x mixture, the concentration of N_2 in the effluent dropped to 125 ppm, while the concentration of NO_x was elevated to 945 ppm. Based on the concentrations of NH_3 and NO_x initially present in the feed, it is evident that the oxidation of NH_3 to NO_x prevails under these conditions, consistent with previous literature reports [51]. Since the addition of O_2 does not completely prevent the formation of N_2, one could still assume that reaction (7) proceeds to a certain extent. However, the likelihood of this SCR-type chemistry taking place in FCC regenerators operating at high temperatures is low, because numerous literature reports indicate that such chemistry typically occurs at temperatures below 400 °C [52–55]. Moreover, a comparison of the data shown in Figs. 4 and 5 for different feed compositions having excess O_2 indicates that the content of N_2 in the effluent is approximately the same regardless of the concentration of NO_x present in the feed, suggesting that the contribution of NO_x species to the N_2 selectivity via reactions (6) and/or (7) is not significant. As a result, it appears that the direct oxidation of NH_3 (reaction (5)) is the primary pathway leading to N_2 in this case. Therefore, reactions (4) and (5) most likely represent the simplified primary network taking place over the $Ce^{n+}/Na^+/\gamma\text{-}Al_2O_3$ material exposed to a 2500 ppm O_2/500 ppm NH_3/He mixture at high temperatures.

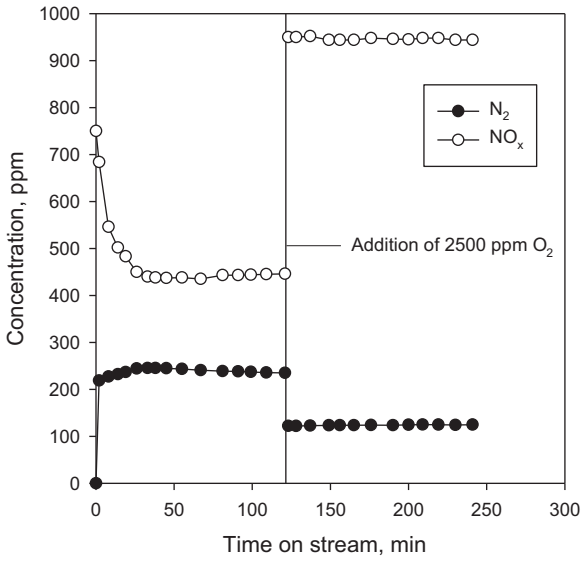

Fig. 5. Reduction of NO_x with NH_3 at 700 °C over the $Ce^{n+}/Na^+/\gamma\text{-}Al_2O_3$ material (feed composition: 500 ppm NH_3/750 ppm NO/He).

A completely different product distribution pattern was observed in the case of the Pd-containing material. In this case, N_2 is selectively formed over the reduced $Pd/Ce^{n+}/Na^+/\gamma\text{-}Al_2O_3$ sample in the 150–300 °C temperature range with a maximum being observed at 300 °C (Fig. 6A). Above this temperature, the formation of N_2 declines, while the NO_x concentration increases and eventually becomes dominant at temperatures above 400 °C. In the 200–500 °C temperature range, relatively small concentrations of N_2O were also detected among the reaction products. This product distribution pattern is consistent with what was reported previously for NH_3 oxidation over (Pd, Pt, or Rh)/Fe/ZSM-5 [56], $Cu/\gamma\text{-}Al_2O_3$ [57], and $PdO/\gamma\text{-}Al_2O_3$ catalysts [58]. The oxidized $Pd^{n+}/Ce^{n+}/Na^+/\gamma\text{-}Al_2O_3$ sample shows a similar product distribution pattern (Fig. 6B), with the N_2, N_2O, and NO_x curves shifted to higher temperatures, consistent with the onset of the NH_3 conversion curve observed for this sample (Fig. 3).

When in separate experiments the Pd-containing samples were exposed to a 500 ppm NH_3/750 ppm NO/He mixture at 700 °C, approximately 94% of NO_x was converted to N_2, indicating that the Pd component catalyzes the reduction of NO_x by NH_3 (Fig. 7).

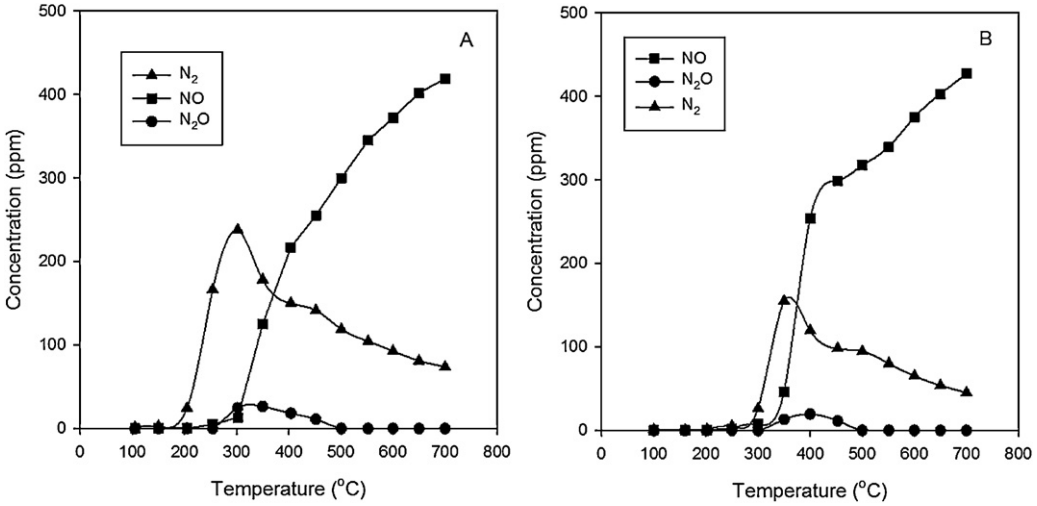

Fig. 6. Product distribution of NH_3 oxidation as a function of temperature over the $Pd^{n+}/Ce^{n+}/Na^+/\gamma\text{-}Al_2O_3$ material treated in H_2 (A) or O_2 (B) at 550 °C (feed composition: 2500 ppm O_2/500 ppm NH_3/He).

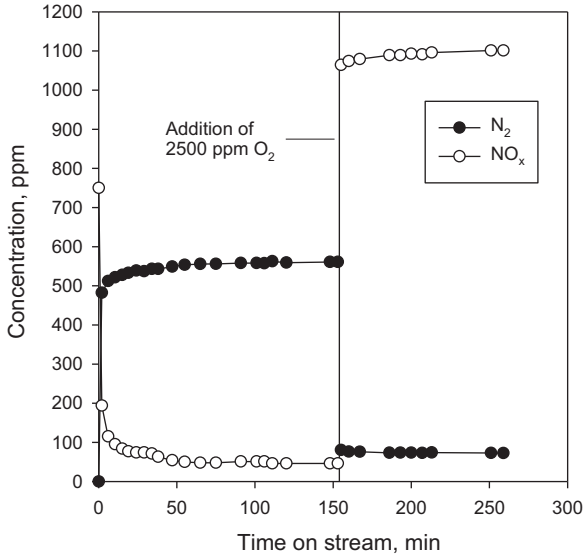

Fig. 7. Reduction of NO_x with NH_3 at 700 °C over the $Pd^{n+}/Ce^{n+}/Na^+/\gamma\text{-}Al_2O_3$ material treated in H_2 at 550 °C (feed composition: 500 ppm NH_3/750 ppm NO/He).

However, the addition of 2500 ppm O_2 to the NH_3/NO_x mixture significantly decreased the amount of N_2 formed, indicating that the NH_3 + NO reaction is not selective in the presence of high O_2 concentrations in the feed even over the Pd-containing sample, which also promotes the NH_3 oxidation to NO_x at higher rates than the $Ce^{n+}/Na^+/\gamma\text{-}Al_2O_3$ support. Therefore, the overall NH_3 oxidation chemistry and product distribution observed in the case of the $Pd/Ce^{n+}/Na^+/\gamma\text{-}Al_2O_3$ samples appears to be described quite accurately by reactions (4) and (5).

It is further evident that both reduced and oxidized Pd-containing samples generate NO_x in significantly larger amounts than the $Ce^{n+}/Na^+/\gamma\text{-}Al_2O_3$ support during NH_3 oxidation at 700 °C (Fig. 8). This comparison indicates that the metal component substantially promotes the oxidation of NH_3 to NO_x (reaction (4)). The differences in NO_x and N_2 selectivities for the oxidized and reduced Pd-containing samples were relatively small (Fig. 8), most likely because exposure during reaction to high temperatures and a highly oxidizing environment eliminates any major differences introduced during pretreatment.

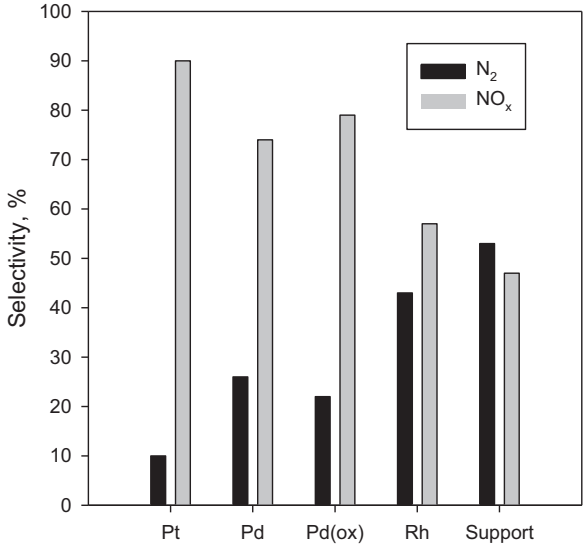

Fig. 8. Comparison of NO_x and N_2 selectivities during NH_3 oxidation at 700 °C over the different $M^{n+}/Ce^{n+}/Na^+/\gamma\text{-}Al_2O_3$ materials treated in H_2 or O_2 (in the case of Pd) at 550 °C (feed composition: 500 ppm NH_3/750 ppm NO/He).

The Pt- and Rh-containing formulations pre-treated in oxygen or hydrogen show the same type of the catalytic behavior for NH_3 oxidation as observed with Pd. While N_2 is selectively formed over these materials at temperatures below 300 °C, NO_x appears in the reaction products at higher temperatures and eventually dominates at temperatures above 400 °C (Figs. 2S and 3S in supporting information). A comparison of NO_x and N_2 selectivities at 700 °C for all noble metals examined is shown in Fig. 8. From this comparison, it becomes evident that all noble metal components promote the formation of NO_x at the expense of N_2, but the selectivities vary depending on the nature of the metal component. As a result, Rh shows the highest selectivity towards N_2, while Pt shows the lowest one. The selectivity pattern observed is consistent with the ability of these metals to catalyze oxidation reactions (in which the order of reactivity declines from Pt to Rh) and correlates with the initial heats of oxygen adsorption on their surfaces, ranging from 275 kJ mol^{-1} for Pt to 312 kJ mol^{-1} for Rh, consistent with the notion that metals with weakly bound oxygen species typically exhibit higher oxidation activity [59].

Since the effective activation of NH_3 on metal surfaces requires the presence of activated oxygen, it has also been suggested that the nature of oxygen species can substantially influence NO_x and N_2 selectivities during NH_3 oxidation [42,60,61]. For example, when this reaction was performed over Pt gauzes in the 700–900 °C temperature range, it was established that weakly bound oxygen species are capable of oxidizing NH_x intermediates to NO_x, while strongly bound oxygen primarily assists in the recombination of NH_x intermediates to from N_2 [61]. It is possible that the same principle can be applicable to the $M/Ce^{n+}/Na^+/\gamma\text{-}Al_2O_3$ samples. The metal component of these materials is expected to be fully oxidized at 700 °C under the highly oxidizing environment used in our experiments. The results of the NH_3 decomposition experiments discussed previously indicate that oxygen incorporated in PdO species participates in the NH_3 decomposition process (reaction (3)). Therefore, for all noble metals examined, the strength of the metal-oxygen bonds in the metal oxide phase is expected to have an effect on the NH_3 oxidation selectivity. Literature data indeed show that standard enthalpy values for the formation of Rh_2O_3, PdO, and PtO species are −119, −116, and −71 kJ mol^{-1}, respectively [63], suggesting that the strength of the metal-oxygen bonds in these oxides follows the trend Rh > Pd > Pt, which is consistent with the increase in the N_2 selectivity from Pt to Rh observed experimentally.

3.3.2. *Oxidation of NH_3 with variable O_2 concentrations*

In an effort to understand how the product distribution of NH_3 oxidation depends on the concentration of oxygen, different O_2/500 ppm NH_3/He feeds containing O_2 concentrations in the 200–1500 ppm range were used. These experiments were performed at 700 °C with the goal of simulating conditions in the various zones within the dense phase of partial burn FCC regenerators. Once again, since the Pt-, Pd-, and Rh-containing samples exhibited similar properties, the results summarized in Fig. 9 provide a comparison for only the $Pd^{n+}/Ce^{n+}/Na^+/\gamma\text{-}Al_2O_3$ and $Ce^{n+}/Na^+/\gamma\text{-}Al_2O_3$ samples. Under these conditions, steady state is reached within a few minutes of exposure to the reaction feed. The results obtained for the $Pd^{n+}/Ce^{n+}/Na^+/\gamma\text{-}Al_2O_3$ sample with 200 ppm O_2 in the feed show NH_3 conversion and N_2 selectivity values of approximately 52 and 100%, respectively (Fig. 9A). When the concentration of O_2 in the feed was increased to 350 ppm, the conversion of NH_3 was also increased to 100%, while the N_2 selectivity remained at the 100% level and no measurable NO_x concentration was detected in the effluent. However, significant changes in the N_2 selectivity were observed when the concentration of O_2 was

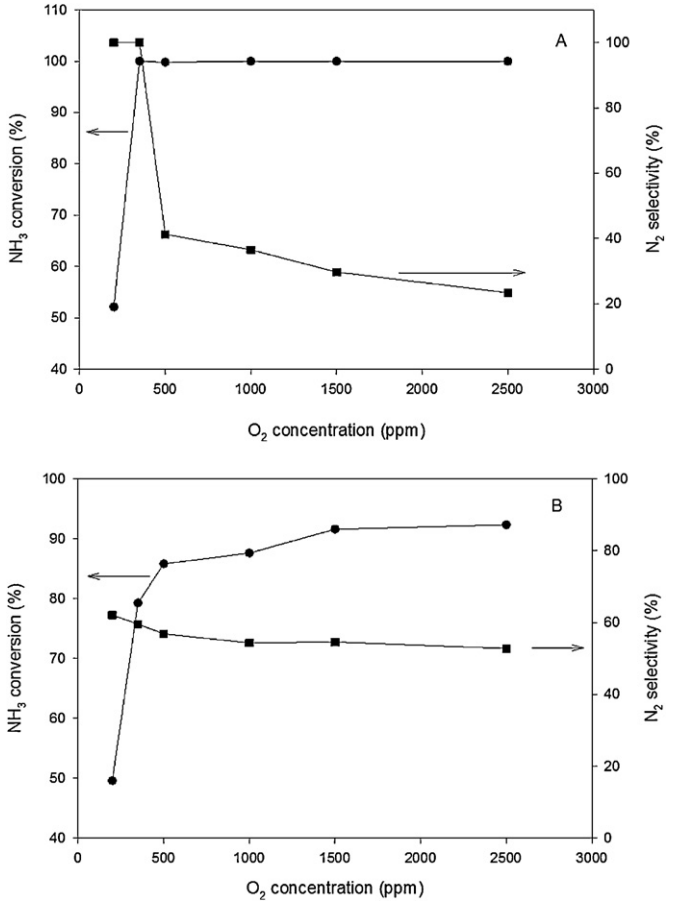

Fig. 9. Conversion of NH_3 and N_2 selectivity as a function of O_2 concentration during NH_3 oxidation at 700 °C over $Pd^{n+}/Ce^{n+}/Na^+/\gamma\text{-}Al_2O_3$ (A) and $Ce^{n+}/Na^+/\gamma\text{-}Al_2O_3$ (B) materials treated in H_2 at 550 °C (feed composition: 200–2500 ppm O_2/500 ppm NH_3/He).

increased beyond this point. For example, when the O_2 concentration was further increased to 500 ppm, the NO_x and N_2 selectivities were found to be 59 and 41%, respectively. The N_2 selectivity continued to decrease with increasing O_2 concentrations, although the changes observed with O_2 concentrations above 500 ppm were smaller, reaching eventually 23% with 2500 ppm O_2 present in the feed (Fig. 9A).

When similar experiments were performed with the $Ce^{n+}/Na^+/\gamma\text{-}Al_2O_3$ support, lower NH_3 conversions were observed, consistent with the activity measurements discussed in the previous sections. However, the N_2 and NO_x selectivities were found to be almost constant (i.e., on the order of 57 and 42%, respectively) regardless of the O_2 concentration in the feed (Fig. 9B).

Several important conclusions can be drawn from this comparison. It is evident from the results that the $Ce^{n+}/Na^+/\gamma\text{-}Al_2O_3$ support exhibits a relatively high activity at 700 °C for NH_3 oxidation to NO_x and N_2 even when the O_2 content in the feed is low. The addition of Pd to the support promotes the conversion of NH_3 in the entire range of O_2 concentrations examined. However, the selectivity of the NH_3 oxidation process over the $Pd^{n+}/Ce^{n+}/Na^+/\gamma\text{-}Al_2O_3$ catalyst depends strongly on the O_2 content. With 500 ppm NH_3 in the feed, there is only a small range of O_2 concentrations (i.e., $\leq$ 350 ppm) in which N_2 is formed with 100% selectivity. Under these conditions, it appears that the Pd component effectively reduces even the NO_x species which are formed over the support surface. Since reactions (4) and (5) are most likely responsible for the formation of N_2 and NO_x on the $Ce^{n+}/Na^+/\gamma\text{-}Al_2O_3$ support, one can calculate that the 350 ppm O_2 in the feed are consumed to reach a NH_3 conversion of 79% and to form the nitrogen-containing products in the concentrations listed in Table 2. With an expected similar contribution of the support to the overall NH_3 oxidation activity of the Pd-containing catalyst, this simply means that the entire amount of NO_x (i.e., 160 ppm) generated by the support is effectively converted to N_2 by reacting with the remaining 104 ppm of NH_3 via reaction (6) to achieve 100% of N_2 selectivity. Indeed, our data show that reaction (6) takes place in the absence of O_2 over both the support and the Pd-containing catalyst (Figs. 5 and 7), but the NO_x conversions are low (i.e., 40%) over the support and close to 94% over the Pd-containing catalyst. Therefore, we can safely infer that with 350 ppm of O_2 in the feed, the $NO + NH_3$ reaction (primarily catalyzed by the Pd component) complements reactions (4) and (5) taking place on the support to yield selectively N_2. Furthermore, one can also estimate that with 500 ppm of NH_3 present, the optimal O_2 concentration in the feed should be on the order of 375 ppm to satisfy the two step $NH_3 - NO_x - N_2$ transformation process leading to 100% of N_2 selectivity, given that all O_2 is consumed during the NH_3 transformation to NO_x at the first step but a sufficient concentration of NH_3 remains to convert all NO_x formed. Excess amounts of O_2 above this optimal level impede this reaction network due to the reaction of O_2 with NH_3 to form NO_x (reaction (4)). Under such circumstances, the lack of NH_3 for reaction (6) largely explains the decrease in N_2 selectivity.

Finally, our results show that the $M^{n+}/Ce^{n+}/Na^+/\gamma\text{-}Al_2O_3$ formulations, which are typically used as CO combustion promoters, are capable of converting NH_3 selectively to N_2 at the high temperatures present in FCC regenerators. Since NO_x species are intermediates in this process, the selective conversion of NH_3 to N_2 takes place only in oxygen deficient zones. It is possible that the presence of such zones, as well as the levels of NH_3 and NO_x formed during the regeneration process can be controlled to some extent by adjusting the O_2 content in the feed. Therefore, at least in principle, optimal operation regimes between partial and full burn conditions can be found to minimize NO_x and NH_3 emissions from FCC regenerators with the use of $M^{n+}/Ce^{n+}/Na^+/\gamma\text{-}Al_2O_3$ combustion promoters.

3.3.3. *Low temperature NH_3 oxidation*

NH_3 conversion curves characterizing the different $M^{n+}/Ce^{n+}/Na^+/\gamma\text{-}Al_2O_3$ catalysts clearly show that these samples are very active for NH_3 oxidation at temperatures below 400 °C (Fig. 3 and Figs. 1S and 3S in supporting information). Since the contribution of the $Ce^{n+}/Na^+/\gamma\text{-}Al_2O_3$ support to the overall activity is negligible in this temperature range, it is evident that the metal component is primarily responsible for the low temperature oxidation activity of these materials. While the product distribution curves were found to be somewhat similar for all three noble metal-containing catalysts examined (Fig. 6 and Figs. 2S and 3S in supporting information), the selectivities to the different products (i.e., N_2, N_2O, and NO_x) varied with temperature, depending on the metal and pretreatment used. N_2 was the primary product of NH_3 oxidation under excess O_2 conditions at temperatures below 400 °C over all three catalysts, while at temperatures below 300 °C NO_x was either present in trace amounts or non-detectable at all. The temperature range in which formation of N_2O species was observed varied with the metal and pretreatment used. In general, N_2O species were formed in smaller amounts and at higher temperatures over oxidized samples than over reduced ones. Moreover, N_2O species were formed in considerably larger amounts over the Pt- and Rh-containing catalysts. As far as the formation of N_2 is concerned, the optimal temperatures at which the maximum yield of N_2 was observed follows the Pt < Pd < Rh order (Fig. 6 and Figs. 2S and 3S in supporting information). Once again, this pattern strongly correlates with the ability of these noble metals to catalyze oxidation reactions in which the order of

Table 2
Product distribution of NH_3 oxidation over different samples at 700 °C (feed composition: 350 ppm O_2/500 ppm NH_3/He).

Sample	Treatment	Products formed (ppm)		NH_3 conversion (%)	Selectivity (%)	
		N_2	NO_x		N_2	NO_x
$Ce^{n+}/Na^+/\gamma$-Al_2O_3	H_2 550 °C	118	160	79	60	40
$Pd/Ce^{n+}/Na^+/\gamma$-Al_2O_3	H_2 550 °C	250	0	100	100	0

reactivity declines from Pt to Rh [40]. Since the temperature ranges for the formation of N_2 and N_2O overlap with each other, the formation of the latter species affects negatively the N_2 selectivity. However, a temperature range can be found for each specific sample in which N_2 is formed selectively and the NH_3 conversion is relatively high.

The catalytic data obtained for the various $M^{n+}/Ce^{n+}/Na^+/\gamma$-$Al_2O_3$ catalysts combined with FTIR results reported elsewhere [19–21] allow us to evaluate possible pathways for the low temperature oxidation of NH_3 over these materials. Several literature reports suggest that the oxidation of NH_3 over γ-Al_2O_3- and zeolite-supported Ag, Pt, Rh, and Pd follows an iSCR-type pathway at low temperatures [62–65]. This pathway includes the oxidation of a significant percentage of NH_3 into NO_x, which then reacts with the remaining NH_3 to form N_2. While the mechanism and the nature of the key intermediates of this pathway are still under discussion, the importance of NH_3 activation on acid sites and the interactions of the activated species thus formed with gas-phase or adsorbed NO_x have been emphasized in the literature [52–55]. However, this acid-catalyzed mechanism is not applicable to the $M^{n+}/Ce^{n+}/Na^+/\gamma$-$Al_2O_3$ catalysts examined in our case because the support itself was found to be inactive for the oxidation of NH_3 at low temperatures.

It has also been suggested that a nitrite mechanism represents an alternative pathway in describing the SCR process [66]. Based on DFT calculations, it has been proposed that the formation of nitrite species is the rate determining step in this mechanism. However, once such species are formed, they can readily react with molecularly adsorbed NH_3 to form N_2. In fact, this mechanism appears to agree well with the experimental results collected for the $M^{n+}/Ce^{n+}/Na^+/\gamma$-$Al_2O_3$ samples. For example, the formation of nitrite/nitrate species on the surface of the $Pd^{n+}/Ce^{n+}/Na^+/\gamma$-$Al_2O_3$ sample after exposure to a NH_3/O_2/He mixture at elevated temperatures was documented by our previous FTIR work [21]. Also, it was established that nitrite/nitrate species thus formed can be completely removed from the surface following subsequent exposure to a NH_3/He mixture, indicating that these species are capable of reacting with NH_3 at elevated temperatures [21]. However, the nature of the products formed during this reaction was not previously identified. In order to do so, the sequence of treatments previously applied during FTIR measurements was repeated in a reactor system with larger amounts of the catalyst used. More specifically, the $Pd^{n+}/Ce^{n+}/Na^+/\gamma$-$Al_2O_3$ sample was first treated in an O_2/He mixture at 550 °C for approximately 2 h to remove any surface bound species, then purged with He at the same temperature, cooled down to 400 °C under the flow of He, and then exposed to a 500 ppm NO/1% O_2/He mixture for 3 h to form surface nitrite/nitrate species in substantial concentrations. When this treatment was completed, the sample was briefly purged with He and exposed to a 500 ppm NH_3/He mixture. The results shown in Fig. 10 indicate that NH_3 quickly reacts with the surface nitrite/nitrate species to produce N_2 in substantial concentrations. When all surface nitrite/nitrate species are consumed, the concentration of N_2 drops to the level observed for a similar sample that was not saturated with nitrite/nitrate species. Both samples show the same steady state behavior thereafter, associated with thermal decomposition/lattice O_2 assisted oxidation of ammonia, as discussed in Section 3.2. Therefore, the combination of the FTIR results reported previously [21] and the current activity measurements reported herein provide strong experimental evidence that NH_3 reacts with nitrite/nitrate species formed on the surface of $M^{n+}/Ce^{n+}/Na^+/\gamma$-$Al_2O_3$ materials to selectively produce N_2. This conclusion is also consistent with a growing body of literature examples documenting a similar type of reaction taking place over surfaces of various catalytic materials having NO_x storage and reduction capabilities [67–70]. For example, it has been reported that NO_x species stored on the surface of Pt-Ba/γ-Al_2O_3 formulations in the form of barium nitrates interact with NH_3 according to the following stoichiometry [67,68]:

$$3Ba(NO_3)_2 + 10NH_3 \rightarrow 8N_2 + 3BaO + 15H_2O \quad (8)$$

Therefore we can conclude with confidence that the main role of the metal component in $M^{n+}/Ce^{n+}/Na^+/\gamma$-$Al_2O_3$ formulations at low temperatures is to effectively oxidize a fraction of NH_3 into NO_x (reaction (4)). As soon as NO_x is formed, it can react with the remaining NH_3 to selectively form N_2 (reaction (7)). Most likely, the latter reaction proceeds via a nitrite/nitrate route in which NO_x is stored on the support surface in the form of surface nitrite/nitrate species first and then reacts with NH_3. The Ce and Na components of the support most likely assist not only in the formation of the nitrite/nitrate species from NO_x but also in their storage, as evidenced by the FTIR results reported elsewhere [19,20]. A balanced contribution from NH_3 oxidation and NO reduction by NH_3 is required to achieve high N_2 selectivities. The results shown in Fig. 6 and Figs. 2S and 3S (supporting information) indicate that this is indeed the case at temperatures below 300 °C, presumably due to the lower rate of the NH_3 oxidation reaction under these conditions. At higher temperatures, however, the N_2 selectivity drops substantially due to the increase in the rate of NH_3 oxidation and therefore, the decreased availability of NH_3 to complete the reduction of NO_x via reaction (7). In addition, several literature reports indicate that nitrates formed on metal oxide surfaces can undergo decomposition at temperatures above 300 °C to produce NO_x and

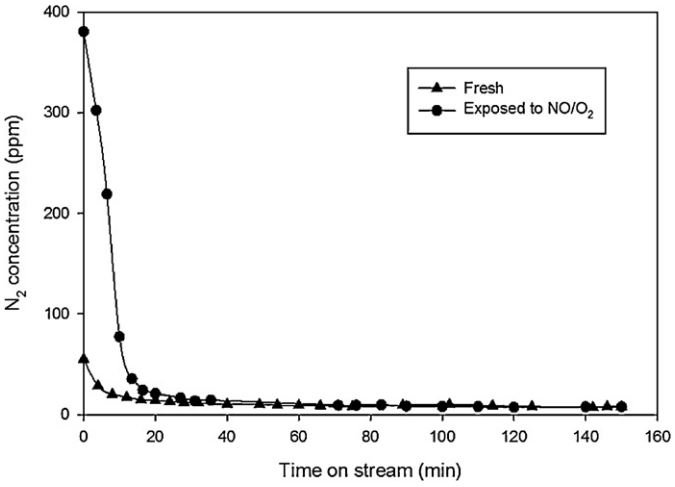

Fig. 10. Concentration of N_2 in the effluent as a function of time during exposure of $Pd^{n+}/Ce^{n+}/Na^+/\gamma$-$Al_2O_3$ to a 500 ppm NH_3/He mixture at 400 °C: (▲) fresh sample and (●) sample treated in a 500 ppm NO/1% O_2/He mixture at 400 °C for 3 h.

O_2 species [71–77]. Such a decomposition of surface nitrite/nitrate species combined with the decreased availability of NH_3 further contributed to the formation of NO_x at temperatures above 300 °C.

4. Conclusions

The reactivity of NH_3 on the surfaces of FCC CO combustion promoters with a $M^{n+}/Ce^{n+}/Na^+/\gamma\text{-}Al_2O_3$ (where M = Pt, Pd, Rh) general composition was examined in a wide range of temperatures in the presence and absence of oxygen. The results obtained provide a strong basis for understanding the NH_3 oxidation chemistry over these materials under different conditions employed in FCC regenerators. All formulations examined were found to be active in promoting the decomposition of NH_3 into N_2 in the 500–700 °C temperature range. However, the Rh-containing formulation was the most active for this process at 700 °C, the temperature which resembles most closely the conditions in FCC regenerators. Oxidized samples were more active than reduced ones, indicating that oxygen species activated on surfaces of these materials significantly enhance the conversion of NH_3 into N_2. In contrast, the reduced formulations were more active and selective for the conversion of NH_3 into N_2 from feeds enriched with O_2, as nearly 100% NH_3 conversions with approximately 80% N_2 selectivity were observed over the reduced Pt-, Pd-, and Rh-containing formulations at temperatures as low as 200, 300, and 350 °C, respectively. In this low temperature region, the NH_3 oxidation reaction follows the iSCR-type pathway in which a significant fraction of NH_3 is first converted into NO_x, which is adsorbed on the catalyst surface in the form of reactive nitrite/nitrate species. In a subsequent step, these nitrite/nitrate surface species react with the remaining NH_3 to form N_2.

The results of activity measurements performed under variable concentrations of O_2 at 700 °C indicate that NO_x is the main product of NH_3 oxidation under these conditions. Moreover, the N_2 selectivity strongly depends on the amount of O_2 in the feed at such high temperatures. However, optimal O_2 concentrations, yielding complete NH_3 conversion and high N_2 selectivity, can be identified for each material. This is possible because the metal component of the $M^{n+}/Ce^{n+}/Na^+/\gamma\text{-}Al_2O_3$ formulations promotes the $NO_x + NH_3$ reaction to form N_2. However, the presence of excess O_2 effectively shuts down this reaction pathway since the oxidation of NH_3 into NO_x prevails under these conditions. In the presence of excess amounts of O_2, the N_2 selectivity strongly depends on the nature of the noble metal used and declines in the Rh > Pd > Pt order. Overall, these results indicate that the significant increase in NO_x emissions typically observed over conventional Pt-based FCC CO combustion promoters is related to the oxidation of NH_3 formed in reducing zones of FCC regenerators.

Acknowledgements

Authors at the University of South Carolina acknowledge partial financial support from the National Science Foundation (Division of Chemical, Bioengineering, Environmental and Transport Systems (CBET); Award ID 0730937).

Appendix A. Supplementary data

Supplementary data associated with this article can be found, in the online version, at http://dx.doi.org/10.1016/j.apcatb.2012.09.057.

References

[1] R.H. Harding, A.W. Peters, J.R.D. Nee, Applied Catalysis A 221 (2001) 389–396.
[2] X. Zhao, A.W. Peteres, G.W. Weatherbee, Industrial and Engineering Chemistry Research 36 (1997) 4535–4542.
[3] D.M. Stockwell, C.P. Kelkar, Studies in Surface Science and Catalysis 149 (2004) 177–188.
[4] G. Yaluris, J.A. Rudesill, US Patent 6,660,683 (2003).
[5] D.M. Stockwell, US Patent 7,678,735 (2010).
[6] S. Schäfer, B. Bonn, Chemie Ingenieur Technik 71 (1999) 613–618.
[7] J.-O. Barth, A. Jentys, J.A. Lercher, Industrial and Engineering Chemistry Research 43 (2004) 3097–3104.
[8] O. Krocher, M. Elsener, Applied Catalysis B 92 (2009) 75–89.
[9] S. Schäfer, B. Bonn, Fuel 81 (2002) 1641–1646.
[10] W-C. Cheng, G. Kim, A.W. Peters, X. Zhao, K. Rajagopalan, Catalysis Reviews: Science and Engineering 40 (1998) 39–79.
[11] K.L. Dishman, P.K. Doolin, L.D. Tullock, Industrial and Engineering Chemistry Research 37 (1998) 4631–4636.
[12] A.W. Peters, E.F. Rakiewicz, G.D. Weatherbee, X. Zhao, U.S. Patent 6,358,881 (2002).
[13] S.M. Krishnamoorthy, M.S. Ziebarth, G. Yaluris, R.J. Lussier, J.A. Rudesill, U.S. Patent 7,976,697 (2011).
[14] A. Peters, X. Zhao, G. Yaluris, S. Davey, A. Karmer, NPRA Annual Meeting, 1998.
[15] E.A. Efthimiadis, E.F. Iliopoulou, A.A. Lappas, D.K. Latridis, I.A. Vasalos, Industrial and Engineering Chemistry Research 41 (2002) 5401–5409.
[16] F.S. Rosser, M.W. Schnaith, P.D. Walker, AIChE Annual Meeting Conference Proceedings, Des Plaines, IL, USA, 2004.
[17] G. Yaluris, J.A. Rudesill, W. Suarez, US Patent 7,307,038 (2007).
[18] G. Yaluris, J.A. Rudesill, US Patent 6,881,390 (2005).
[19] O.S. Alexeev, S. Krishnamoorthy, M.S. Ziebarth, G. Yaluris, T.G. Roberie, M.D. Amiridis, Catalysis Today 127 (2007) 176–188.
[20] O.S. Alexeev, S. Krishnamoorthy, C. Jensen, M.S. Ziebarth, G. Yaluris, T.G. Roberie, M.D. Amiridis, Catalysis Today 127 (2007) 189–198.
[21] B. Bahrami, V.G. Komvokis, U. Singh, M.S. Ziebarth, O.S. Alexeev, M.D. Amiridis, Applied Catalysis A 391 (2011) 11–21.
[22] L. Li, Z.H. Zhu, S.B. Wang, X.D. Yao, Z.F. Yan, Journal of Molecular Catalysis A 304 (2009) 71–76.
[23] A. Ogata, K. Mizuno, S. Kushiyama, T. Yamamoto, Plasma Chemistry and Plasma Processing 18 (1998) 363–373.
[24] R.K. Grasselli, Topics in Catalysis 21 (2002) 79–88.
[25] Y. Kosaki, A. Miyamoto, Y. Murakami, Bulletin of the Chemical Society of Japan 52 (1979) 617–618.
[26] A. Miyamoto, Y. Kosaki, Y. Murakami, Chemistry Letters (1978) 397–400.
[27] J.C. Ganley, F.S. Thomas, E.G. Seebauer, R.I. Masel, Catalysis Letters 96 (2004) 117–122.
[28] G. Papapolymerou, V. Bontozoglou, Journal of Molecular Catalysis A 120 (1997) 165–171.
[29] G. Novell-Leruth, A. Valcarcel, J. Pérez-Ramírez, J.M. Ricart, Journal of Physical Chemistry C 111 (2007) 860–868.
[30] H.H. Kung, Transition Metal Oxides: Surface Chemistry and Catalysis, vol. 45, Elsevier, Amsterdam, 1991.
[31] H. Imagawa, A. Suda, K. Yamamura, S. Sun, Journal of Physical Chemistry C 115 (2011) 1740–1745.
[32] E.V. Kondratenko, O. Buyevskaya, M. Baerns, Journal of Molecular Catalysis A 158 (2000) 199–208.
[33] E.V. Kondratenko, O. Buyevskaya, M. Baerns, Catalysis Letters 63 (1999) 153–159.
[34] A. Galtayries, E. Laksono, J.-M. Siffre, C. Argile, P. Marcus, Surface and Interface Analysis 30 (2000) 140–144.
[35] K. Kusakabe, K. Harada, Y. Ikuno, H. Nagara, Journal of Physics: Condensed Matter 21 (2009) 1–7.
[36] L. Gang, J. van Grondelle, B.G. Anderson, R.A. van Santen, Journal of Catalysis 186 (1999) 100–109.
[37] R. Zhou, B. Zhao, B. Yue, Applied Surface Science 254 (2008) 4701–4707.
[38] X. Zhanga, E. Longa, Y. Li, L. Zhangb, J. Guoc, M. Gonga, Y. Chena, Journal of Molecular Catalysis A 308 (2009) 73–78.
[39] L.S.F. Feio, C.E. Hori, S. Damyanova, F.B. Noronha, W.H. Cassinelli, C.M.P. Marques, J.M.C. Bueno, Applied Catalysis A 316 (2007) 107–116.
[40] Y. Li, J.N. Armor, Applied Catalysis B 13 (1997) 131–139.
[41] E.V. Kondratenko, V.A. Kondratenko, M. Richter, R. Fricke, Journal of Catalysis 239 (2006) 23–33.
[42] V.A. Kondratenko, U. Bentrup, M. Richter, T.W. Hansen, E.V. Kondratenko, Applied Catalysis B 84 (2008) 497–504.
[43] M. Lyubovsky, L. Pfefferle, Catalysis Today 47 (1999) 29–44.
[44] R.F. Hicks, H. Qi, M.L. Young, R.G. Lee, Journal of Catalysis 122 (1990) 280–294.
[45] R.F. Hicks, H. Qi, M.L. Young, R.G. Lee, Journal of Catalysis 122 (1990) 295–306.
[46] C.A. Muller, M. Maciejewski, R.A. Koeppel, A. Baiker, Catalysis Today 47 (1999) 245–252.
[47] M. Mavrikakis, Y. Xu, Fuel Chemistry Division Preprints 47 (2002) 223–225.
[48] A. Eichler, F. Mittendorfer, J. Hafner, Journal of Physical Review B 62 (2000) 4744–4755.
[49] A. Groß, A. Eichler, J. Hafner, M.J. Mehl, D.A. Papaconstantopoulos, Surface Science 539 (2003) L542–L548.
[50] M.K. Rose, A. Borg, J.C. Dunphy, T. Mitsui, D.F. Ogletree, M. Salmeron, Surface Science 547 (2003) 162–170.
[51] J.M. Watson, U.S. Ozkan, Journal of Molecular Catalysis A 192 (2003) 79–91.
[52] G. Busca, L. Lietti, G. Ramis, F. Berti, Applied Catalysis B 18 (1998) 1–36.
[53] S. Djerad, M. Crocoll, S. Kureti, L. Tifouti, W. Weisweiler, Catalysis Today 113 (2006) 208–214.
[54] H. Sjovall, L. Olsson, E. Fridell, R.J. Blint, Applied Catalysis B 64 (2006) 180–188.

[55] W.E.J. Van Kooten, B. Liang, H.C. Krijnsen, O.L. Oudshoorn, H.P.A. Calis, C.M. van den Bleek, Applied Catalysis B 21 (1999) 203–213.
[56] R.Q. Long, R.T. Yang, Catalysis Letters 78 (2002) 353–357.
[57] A.R. Sirdeshpande, J.S. Lighty, Industrial and Engineering Chemistry Research 39 (2000) 1781–1787.
[58] L. Lietti, C. Ramella, G. Groppi, P. Forzatti, Applied Catalysis B 21 (1999) 89–101.
[59] J.J. Spivey, Catalysis, vol. 17, Royal Society of Chemistry, Cambridge, 2004.
[60] J. Pérez-Ramırez, E.V. Kondratenko, V.A. Kondratenko, M. Baerns, Journal of Catalysis 227 (2004) 90–100.
[61] G.V. Samsonov, The Oxide Handbook, second ed., IFI/Plenum, New York, 1982.
[62] L. Zhang, H. He, Journal of Catalysis 268 (2009) 18–25.
[63] L. Chmielarz, P. Kustrowski, A. Rafalska-Lasocha, R. Dziembaj, Applied Catalysis B 58 (2005) 235–244.
[64] G. Oi, J.E. Gatt, R.T. Yang, Journal of Catalysis 226 (2004) 120–128.
[65] L. Gang, B.G. Anderson, J. van Grondelle, R.A. van Santen, Applied Catalysis B 40 (2003) 101–110.
[66] R. Yuan, G. Fu, X. Xu, H. Wan, Physical Chemistry Chemical Physics 13 (2011) 453–460.
[67] P. Forzatti, L. Lietti, I. Nova, Energy and Environmental Science 1 (2008) 236–247.
[68] L. Lietti, I. Nova, P. Forzatti, Journal of Catalysis 257 (2008) 270–282.
[69] C. Ciardelli, I. Nova, E. Tronconi, D. Chatterjee, B. Bandl-Konrad, M. Weibel, B. Krutzsch, Applied Catalysis B 70 (2007) 80–90.
[70] A. Grossale, I. Nova, E. Tronconi, D. Chatterjee, M. Weibel, Journal of Catalysis 256 (2008) 312–322.
[71] X. Zhang, H. He, H. Gao, Y. Yu, Spectrochimica Acta Part A 71 (2008) 1446–1451.
[72] A. Setiabudi, J. Chen, G. Mul, M. Makkee, J.A. Moulijn, Applied Catalysis B 51 (2004) 9–19.
[73] S. Suárez, J.A. Martín, M. Yates, P. Avila, J. Blanco, Journal of Catalysis 229 (2005) 227–236.
[74] C.B. Wang, J.G. Chang, R.C. Wu, C.T. Yeh, Applied Catalysis B 17 (1998) 51–62.
[75] M. Piacentini, M. Maciejewski, A. Baiker, Applied Catalysis B 72 (2007) 105–117.
[76] S. Benard, L. Retailleau, F. Gaillard, P. Vernoux, A. Giroir-Fendler, Applied Catalysis B 55 (2005) 11–21.
[77] B.A. Silletti, R.T. Adams, S.M. Sigmon, A. Nikolopoulos, J.J. Spivey, H.H. Lamb, Catalysis Today 114 (2006) 64–71.